Mechanics of Composite Materials, Vol. 53, No. 1, March, 2017 (Russian Original Vol. 53, No. 1, January-February, 2017)

THREE-DIMENSIONAL SOLUTION OF THE FREE VIBRATION PROBLEM FOR METAL-CERAMIC SHELLS USING THE METHOD OF SAMPLING SURFACES

G. M. Kulikov* **and S. V. Plotnikova**

Keywords: *metal-ceramic shell, elasticity theory, free vibrations, method of sampling surfaces*

The possibility of using the method of sampling surfaces (SaS) for solving the free vibration problem of three-dimensional elasticity for metal-ceramic shells is studied. According to this method, in the shell body, an arbitrary number of SaS parallel to its middle surface are selected in order to take displacements of these surfaces as unknowns. The SaS pass through the nodes of a Chebyshev polynomial, which improves the convergence of the SaS method significantly. As a result, the SaS method can be used to obtain analytical solutions of the vibration problem for metal-ceramic plates and cylindrical shells that asymptotically approach the exact solutions of elasticity as the number of SaS tends to infinity.

Introduction

In the literature, several approaches to finding analytical solutions to the static and dynamic problems of elasticity theory for composite plates and shells made of functional materials are known: the first is based the application of asymptotic methods [1-3], the second approach is connected with the use of power series in 3D approximations of required functions and elastic constants [4, 5], and the third one is based on the method of 3D states [6, 7]. We should note that the last approach provides an exact solution to a 3D problem of elasticity theory only if the mechanical characteristics of material are distributed across the plate thickness exponentially. The current status of the problem has been discussed in reviews [8-10].

Tambov State Technical University, Russia
*Corresponding author; e-mail: gmkulikov@mail.ru

Translated from Mekhanika Kompozitnykh Materialov, Vol. 53, No. 1, pp. 47-64, January-February, 2017. Original article submitted May 12, 2016.

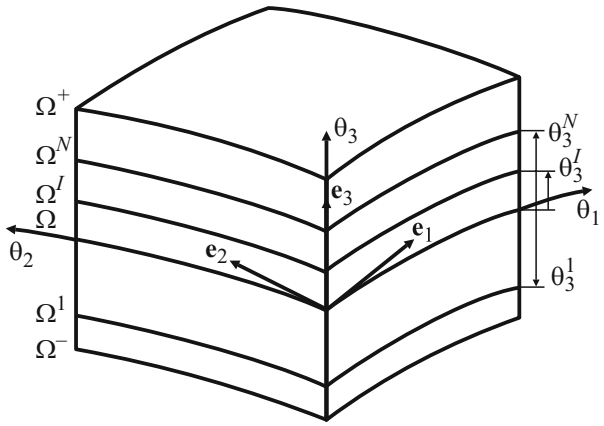

Fig. 1. Arrangement of sampling surfaces in a shell.

In the given work, for solving the 3D problem on free transverse vibrations of a shell made of a functional material, the method of sampling surfaces [11-13] is used, according to which, in the shell body, N sampling surfaces (SaS) $\Omega^1, \Omega^2, ..., \Omega^N$ parallel to its median surface are selected in order to use the displacement vectors $\mathbf{u}^1, \mathbf{u}^2, ..., \mathbf{u}^N$ of these surfaces as required functions. Such a choice of required functions, with a subsequent application of Lagrange polynomials of degree $N-1$ in the 3D approximations of displacements and mechanical characteristics of the material, allows one to present the resolving equations of the high-order theory of shells suggested in a compact form and to construct deformation relations that exactly represent motions of the shell as a rigid body in the system of curvilinear surface coordinates [14].

The high-order theory of shells [11-13] is based on the use of equidistant sampling surfaces, with shell faces taken as reference surfaces. This limits the application of the given theory to calculations of thick shells. The matter is that the suggested 3D polynomial interpolation of displacements with the use of high-degree Lagrange polynomials can result, because of the Runge phenomenon, in significant oscillations of polynomial approximations in the zone of edge effect. With increasing degree of a polynomial, the interpolation error can tend to infinity. In a numerical analysis, to control this phenomenon, the roots of a Chebyshev polynomial are assumed as interpolation nodes [15], which helps one to considerably improve the behavior of high-degree polynomial approximations, whose interpolation error uniformly tends to zero as $N \to \infty$. This makes it possible to find a solution to 3D problems of statics for composite rectangular plates and cylindrical shells made of functional materials [16-19] with any prescribed accuracy, because the analytical solutions asymptotically approach the exact solutions of 3D elasticity theory.

Kinematics of a Shell and Its Deformation Relations

Let us consider a shell of constant thickness h. Its median surface Ω is related to curvilinear orthogonal coordinates θ_1 and θ_2 counted along the lines of principal curvatures, and the θ_3 coordinate is counted in the transverse direction. Let $\mathbf{e}_\alpha$ be the unit vectors of tangents to the coordinate lines θ_α, $\mathbf{e}_3$ — the unit vector of external normal to the median surface, A_α — coefficients of the first quadratic form, k_α — the principal curvatures, $c_\alpha = 1 + k_\alpha \theta_3$ — components of the geometrical tensor of shift, $c_\alpha^I = c_\alpha(\theta_3^I) = 1 + k_\alpha \theta_3^I$ — components of the geometrical tensor of shift on the sampling surfaces Ω^I (Fig. 1), u_i — components of the displacement vector in the basis $\mathbf{e}_i$, $u_i^I = u_i(\theta_3^I)$ — displacements of sampling surfaces, and θ_3^I — transverse coordinates of the surfaces Ω^I located inside the interval $(-h/2,\ h/2)$ and passing through the roots of an Nth-degree Chebyshev polynomial; these coordinates are determined by the formula [15]

$$\theta_3^I = -\frac{h}{2}\cos\left(\pi \frac{2I-1}{2N}\right). \tag{1}$$

Hereinafter, the superscripts I, J, and K indicate that the corresponding quantity belongs to a sampling surface and take the values $1,2,...,N$; the Greek subscripts $\alpha,\beta=1,2;$ the Latin subscripts $i,j,k,l=1,2,3$. We should note that summation over Latin subscripts repeated twice is used in this work.

Components of the strain tensor on sampling surfaces, $\varepsilon_{ij}^I=\varepsilon_{ij}(\theta_3^I)$, can be presented as [18]

$$2\varepsilon_{\alpha\beta}^I=\frac{1}{c_\beta^I}\lambda_{\alpha\beta}^I+\frac{1}{c_\alpha^I}\lambda_{\beta\alpha}^I,\quad 2\varepsilon_{\alpha 3}^I=\beta_\alpha^I+\frac{1}{c_\alpha^I}\lambda_{3\alpha}^I,\quad \varepsilon_{33}^I=\beta_3^I, \tag{2}$$

$$\beta_i^I=u_{i,3}(\theta_3^I), \tag{3}$$

where β_i^I are derivatives of displacements with respect to θ_3 on a sampling surface; $\lambda_{i\alpha}^I$ are deformation parameters of sampling surfaces [18]:

$$\lambda_{\alpha\alpha}^I=\frac{1}{A_\alpha}u_{\alpha,\alpha}^I+B_\alpha u_\beta^I+k_\alpha u_3^I,\quad \lambda_{\beta\alpha}^I=\frac{1}{A_\alpha}u_{\beta,\alpha}^I-B_\alpha u_\alpha^I\quad(\beta\neq\alpha), \tag{4}$$

$$\lambda_{3\alpha}^I=\frac{1}{A_\alpha}u_{3,\alpha}^I-k_\alpha u_\alpha^I,\quad B_\alpha=\frac{1}{A_\alpha A_\beta}A_{\alpha,\beta}\quad(\beta\neq\alpha).$$

Up to this moment, no assumptions have been made for the distribution of displacement and strain fields across the shell thickness. Now, we assume that they are distributed according to the laws [14]

$$u_i=\sum_I L^I u_i^I, \tag{5}$$

$$\varepsilon_{ij}=\sum_I L^I\varepsilon_{ij}^I, \tag{6}$$

where $L^I\left(\theta_3\right)$ are the Lagrange polynomials of degree $N-1$,

$$L^I=\prod_{J\neq I}\frac{\theta_3-\theta_3^J}{\theta_3^I-\theta_3^J}. \tag{7}$$

From Eqs. (3) and (5), it follows that

$$\beta_i^I=\sum_J M^J(\theta_3^I)u_i^J, \tag{8}$$

where $M^J=L_{,3}^J$ are polynomials of degree $N-2$, whose values on the sampling surfaces Ω^I are found from the formulas

$$\begin{gathered}M^J\left(\theta_3^I\right)=\frac{1}{\theta_3^J-\theta_3^I}\prod_{K\neq I,J}\frac{\theta_3^I-\theta_3^K}{\theta_3^J-\theta_3^K}\quad(J\neq I),\\ M^I\left(\theta_3^I\right)=-\sum_{J\neq I}M^J\left(\theta_3^I\right).\end{gathered} \tag{9}$$

Thus, the governing functions β_i^I of the given high-order theory of shells are presented, according to Eq. (8), as a linear combination of displacements u_i^J of sampling surfaces.

We should note that deformation relations (2), with account of Eqs. (4) and (8), exactly represent displacements of the shell as a rigid body in the system of curvilinear surface coordinates. A proof of this fundamental statement is given in [14].

Variational Formulation of the Problem

Let us take advantage of the Hamilton of principle, which, in the case of free vibrations of a shell in the absence of external loads on its faces, can be presented as

$$\delta \int_{t_1}^{t_2} (T - U)\, dt = 0, \tag{10}$$

$$U = \frac{1}{2} \iint_{\Omega} \int_{-h/2}^{h/2} \sigma_{ij} \varepsilon_{ij} A_1 A_2 c_1 c_2 d\theta_1 d\theta_2 d\theta_3, \tag{11}$$

$$T = \frac{1}{2} \iint_{\Omega} \int_{-h/2}^{h/2} \rho \dot{u}_i \dot{u}_i A_1 A_2 c_1 c_2 d\theta_1 d\theta_2 d\theta_3, \tag{12}$$

where U is the internal energy of the shell, T is the kinetic energy, σ_{ij} are stresses, ρ is the specific density, and $\dot{u}_i$ are the derivatives of displacements with respect to time t.

Inserting the distribution (6) of strains across the shell thickness into functional (11) and introducing the resulting stresses

$$H_{ij}^I = \int_{-h/2}^{h/2} \sigma_{ij} L^I c_1 c_2 d\theta_3, \tag{13}$$

we have

$$U = \frac{1}{2} \iint_{\Omega} \sum_I H_{ij}^I \varepsilon_{ij}^I \, A_1 A_2 d\theta_1 d\theta_2. \tag{14}$$

We will restrict our consideration to linearly elastic materials obeying Hooke's law

$$\sigma_{ij} = C_{ijkl} \varepsilon_{kl}, \tag{15}$$

where C_{ijkl} are the elastic moduli of shell material.

The following step consists in choosing a distribution law for the mechanical characteristics of the shell across its thickness. It is obvious, that this distribution in the transverse direction have to agree with the distributions of displacements (5) and strains (6), i.e., we have

$$C_{ijkl} = \sum_I L^I C_{ijkl}^I, \tag{16}$$

$$\rho = \sum_I L^I \rho^I, \tag{17}$$

where $C_{ijkl}^I = C_{ijkl}(\theta_3^I)$ and $\rho^I = \rho(\theta_3^I)$ are the elastic moduli and material densities on the sampling surfaces.

Introducing stresses (15) into Eqs. (13) and (14) and considering the distributions of strains (6) and elastic constants (16) across the shell thickness, we found the expression for the internal energy

$$U = \frac{1}{2} \iint_{\Omega} \sum_I \sum_J \sum_K \Lambda^{IJK} \varepsilon_{ij}^I C_{ijkl}^J \varepsilon_{kl}^K A_1 A_2 d\theta_1 d\theta_2, \tag{18}$$

where

$$\Lambda^{IJK} = \int_{-h/2}^{h/2} L^I L^J L^K c_1 c_2 d\theta_3. \tag{19}$$

Inserting the distributions of displacements (5) and densities (17) across the shell thickness into Eq. (12), we come to the formula for the kinetic energy

$$T = \frac{1}{2}\iint\limits_{\Omega}\sum_{I}\sum_{J}\sum_{K}\Lambda^{IJK}\dot{u}_i^I\rho^J\dot{u}_i^K A_1A_2d\theta_1d\theta_2, \tag{20}$$

Mechanical Characteristics of a Metal-Ceramic Composite

Let us consider a composite with a metal matrix and randomly oriented discrete ceramic inclusions functioning as reinforcing elements. For the elastic moduli, shear moduli, Poisson ratios, and densities of metal and ceramics, the standard designations $E_{\mathrm{m}}, G_{\mathrm{m}}, \nu_{\mathrm{m}}, \rho_{\mathrm{m}}$ and $E_{\mathrm{c}}, G_{\mathrm{c}}, \nu_{\mathrm{c}}, \rho_{\mathrm{c}}$, respectively, will be used.

To describe the mechanical characteristics of a metal-ceramic composite, the following three basic models can be used.

1. *The law of mixtures.* In this model, the elastic constants and density are determined from the formulas [9]

$$E = E_{\mathrm{m}}V_{\mathrm{m}} + E_{\mathrm{c}}V_{\mathrm{c}}, \quad \nu = \nu_{\mathrm{m}}V_{\mathrm{m}} + \nu_{\mathrm{c}}V_{\mathrm{c}}, \tag{21}$$

$$\rho = \rho_{\mathrm{m}}V_{\mathrm{m}} + \rho_{\mathrm{c}}V_{\mathrm{c}}. \tag{22}$$

Here, V_{m} and V_{c} are the volume contents of metal and ceramics, varying across the shell thickness according to a power law [8]:

$$V_{\mathrm{m}} = 1 - V_{\mathrm{c}}, \quad V_{\mathrm{c}} = V_{\mathrm{c}}^{-} + (V_{\mathrm{c}}^{+} - V_{\mathrm{c}}^{-})(h/2 + \theta_3)^{\gamma}, \tag{23}$$

where V_{c}^{-} and V_{c}^{+} are the volume contents of ceramics on shell faces.

2. *Mori–Tanaka model.* Here, the effective elastic moduli of a metal-ceramic composite is determined by the formulas [20, 21]

$$K = K_{\mathrm{m}} + \frac{V_{\mathrm{c}}(K_{\mathrm{c}} - K_{\mathrm{m}})}{1 + V_{\mathrm{m}}(K_{\mathrm{c}} - K_{\mathrm{m}})/(K_{\mathrm{m}} + 4G_{\mathrm{m}}/3)},$$

$$G = G_{\mathrm{m}} + \frac{V_{\mathrm{c}}(G_{\mathrm{c}} - G_{\mathrm{m}})}{1 + V_{\mathrm{m}}(G_{\mathrm{c}} - G_{\mathrm{m}})/(G_{\mathrm{m}} + f_{\mathrm{m}})}, \quad f_{\mathrm{m}} = \frac{G_{\mathrm{m}}(9K_{\mathrm{m}} + 8G_{\mathrm{m}})}{6(K_{\mathrm{m}} + 2G_{\mathrm{m}})}, \tag{24}$$

$$K_{\mathrm{m}} = \frac{E_{\mathrm{m}}}{3(1 - 2\nu_{\mathrm{m}})}, \quad K_{\mathrm{c}} = \frac{E_{\mathrm{c}}}{3(1 - 2\nu_{\mathrm{c}})},$$

where K_{m} and K_{c} are the bulk moduli of elasticity of metal and ceramics, respectively. The density of the composite material can be found by the rule of mixtures, (22) and (23).

3. *The self-consistent Hill model.* According to this model, the effective elastic moduli of a composite material are found by the formulas given in [22]. In this method, first the following fourth-degree equation is solved for the shear modulus G:

$$\frac{V_{\mathrm{m}}K_{\mathrm{m}}}{K_{\mathrm{m}} + 4G/3} + \frac{V_{\mathrm{c}}K_{\mathrm{c}}}{K_{\mathrm{c}} + 4G/3} + 5\left(\frac{V_{\mathrm{m}}G_{\mathrm{c}}}{G - G_{\mathrm{c}}} + \frac{V_{\mathrm{c}}G_{\mathrm{m}}}{G - G_{\mathrm{m}}}\right) + 2 = 0, \tag{25}$$

which has only one positive root. Then, the bulk modulus of elasticity

$$K = \left(\frac{V_{\mathrm{m}}}{K_{\mathrm{m}} + 4G/3} + \frac{V_{\mathrm{c}}}{K_{\mathrm{c}} + 4G/3}\right)^{-1} - 4G/3. \tag{26}$$

is calculated. The density of the material is also determine by the rule of mixtures, (22) and (23).

Analytical Solution of the Problem on Free Vibrations of a Cylindrical Shell

Let us consider free vibrations of a hinge-supported cylindrical metal-ceramic panel of radius R with sides a and $b = \varphi R$, where φ is its central angle. The median surface of the shall is related to curvilinear coordinates θ_1 and θ_2, counted in the longitudinal and circumferential directions, respectively.

The boundary conditions for the hinge-supported cylindrical panel are

$$\sigma_{11} = u_2 = u_3 = 0 \text{ at } \theta_1 = 0, a, \qquad \sigma_{22} = u_1 = u_3 = 0 \text{ at } \theta_2 = 0, b. \tag{27}$$

To satisfy conditions (27), the solution of the problem is sought in the form

$$u_1^I = u_{1rs}^I \mathrm{e}^{\mathrm{i}\omega_{rs}t} \cos\frac{r\pi\theta_1}{a}\sin\frac{s\pi\theta_2}{b}, \quad u_2^I = u_{2rs}^I \mathrm{e}^{\mathrm{i}\omega_{rs}t} \sin\frac{r\pi\theta_1}{a}\cos\frac{s\pi\theta_2}{b},$$
$$u_3^I = u_{3rs}^I \mathrm{e}^{\mathrm{i}\omega_{rs}t} \sin\frac{r\pi\theta_1}{a}\sin\frac{s\pi\theta_2}{b}, \tag{28}$$

where r and s are the numbers of half-waves in the longitudinal and circumferential directions, respectively; u_{irs}^I are the displacements of sampling surfaces, ω_{rs} are eigenfrequencies, and $\mathrm{i} = \sqrt{-1}$ is the imaginary unit.

Introducing displacements (28) into Eqs. (2), (4), (8), (18), and (20) and using Hamilton principle (10), we come to the homogeneous system of linear equations of order $3N$

$$\frac{\partial(T-U)}{\partial \mathbf{W}_{rs}} = 0, \tag{29}$$

where

$$\mathbf{W}_{rs} = \left[u_{1rs}^1 \; u_{1rs}^2 \ldots u_{1rs}^N \; u_{2rs}^1 \; u_{2rs}^2 \ldots u_{2rs}^N \; u_{3rs}^1 \; u_{3rs}^2 \ldots u_{3rs}^N \right]^{\mathrm{T}}. \tag{30}$$

The system of Eqs. (29) can be presented in the matrix form (no summation over the repeating subscripts)

$$(\mathbf{K}_{rs} - \omega_{rs}^2 \mathbf{M}_{rs})\mathbf{W}_{rs} = 0. \tag{31}$$

As is known, the system of Eqs. (31) has a nontrivial solution if

$$\det(\mathbf{K}_{rs} - \omega_{rs}^2 \mathbf{M}_{rs}) = 0, \tag{32}$$

where $\mathbf{K}_{rs}$ and $\mathbf{M}_{rs}$ are the matrices of rigidity and weights of order $3N \times 3N$.

Solving polynomial equation (32), the eigenfrequencies $0 < \omega_{rs}^{(1)} < \omega_{rs}^{(2)} < \ldots < \omega_{rs}^{(3N)}$ are found. The eigenvectors $\mathbf{W}_{rs}^{(q)}$ corresponding to the eigenvalues $\lambda_{rs}^{(q)} = (\omega_{rs}^{(q)})^2$ are determined by solving the homogeneous system of equations (31), where $q = 1, 2, \ldots, 3N$.

The algorithm described was realized in MATLAB with the use of the ToolBox Symbolic Math package, allowing one to carry out symbolic calculations. As a result, an analytical solution to the problem on free vibrations of a metal-ceramic cylindrical panel was found on the basis of the high-order theory of shells suggested. This solution asymptotically approaches the exact solution of the 3D elasticity theory as the number sampling surfaces tends to infinity.

TABLE 1. Calculation Results for the Basic Frequency $\bar{\omega}_{11}^{(1)}$ of Cylindrical Metal-Ceramic Shells

N	$R/h = 5$		$R/h = 10$		$R/h = 100$	
	$\gamma = 2$	$\gamma = 10$	$\gamma = 2$	$\gamma = 10$	$\gamma = 2$	$\gamma = 10$
3	48.5448196367	38.6626974059	34.7299559128	28.5340120780	27.3903742838	23.3961186465
7	48.5250135749	37.8411160800	34.6868917363	28.5678595952	27.3258370621	23.9835886220
11	48.5250115759	37.8402385577	34.6868869163	28.5675534143	27.3258291807	23.9833661714
15	48.5250115765	37.8402382052	34.6868869136	28.5675525827	27.3258291768	23.9833647787
19	48.5250115759	37.8402381975	34.6868869155	28.5675525618	27.3258291767	23.9833647458
23	48.5250115763	37.8402381950	34.6868869084	28.5675525635	27.3258291795	23.9833647453
[23]	48.5250	37.8401	34.6869	28.5673	27.3258	23.9832

TABLE 2. Calculation Results for a Cylindrical Metal-Ceramic Shell with $R/h = 10$, $\gamma = 2$, and $r = s = q = 1$

N	$\bar{u}_1(0.5)$	$\bar{\sigma}_{11}(-0.5)$	$\bar{\sigma}_{11}(0.5)$	$\bar{\sigma}_{12}(0.5)$	$\bar{\sigma}_{13}(0)$	$\bar{\sigma}_{33}(0)$
3	–1.676197780	–4.343370900	36.73051355	2.100743963	1.180502642	–2.499993522
7	–1.675026226	–6.018010121	38.72665137	1.200919408	1.544099953	–4.643783660
11	–1.675026063	–6.021347419	38.72348966	1.200720309	1.539701635	–4.619952481
15	–1.675026056	–6.021264744	38.72354703	1.200722212	1.539776696	–4.620346739
19	–1.675026056	–6.021261910	38.72353471	1.200722088	1.539774593	–4.620319637
23	–1.675026054	–6.021259966	38.72352990	1.200722061	1.539774228	–4.620311690

Numerical Results and Their Discussion

As an example, we will consider the calculation of a cylindrical metal-ceramic panel with geometrical parameters $a = b = 1$ m and $h = 0.1$ m. The mechanical characteristics of panel materials were taken from [23]: $E_{\mathrm{m}} = 7 \cdot 10^{10}$ Pa, $\nu_{\mathrm{m}} = 0.3$, $\rho_{\mathrm{m}} = 2707$ kg/m^3, $E_{\mathrm{c}} = 38 \cdot 10^{10}$ Pa, $\nu_{\mathrm{c}} = 0.3$, $\rho_{\mathrm{c}} = 3000$ kg/m^3, $V_{\mathrm{c}}^{-} = 0$, and $V_{\mathrm{c}}^{+} = 1$. Let us introduce the dimensionless quantities

$$\bar{\omega} = \omega a^2 \sqrt{h\rho_{\mathrm{m}} / D_{\mathrm{m}}}, \quad \bar{u}_1 = u_1(0, b/2s, z)a / hu_3^*, \quad \bar{u}_3 = u_3(a/2r, b/2s, z)/u_3^*,$$

$$\bar{\sigma}_{11} = \sigma_{11}(a/2r, b/2s, z)a^2 / E_{\mathrm{m}} hu_3^*, \quad \bar{\sigma}_{12} = \sigma_{12}(0,0,z)a^2 / E_{\mathrm{m}} hu_3^*,$$

$$\bar{\sigma}_{13} = \sigma_{13}(0, b/2s, z)a^3 / 10E_{\mathrm{m}} h^2 u_3^*, \quad \bar{\sigma}_{33} = \sigma_{33}(a/2r, b/2s, z)a^4 / 10E_{\mathrm{m}} h^3 u_3^*,$$

$$u_3^* = u_3(a/2r, b/2s, 0), \quad D_{\mathrm{m}} = E_{\mathrm{m}} h^3 / 12(1 - \nu_{\mathrm{m}}^2),$$

where $z = \theta_3 / h$ is the dimensionless transverse coordinate.

First, we will analyze the free vibrations of the shell on the basis of the elementary model of mixtures. Calculation results for the basic frequency $\bar{\omega}_{11}^{(1)}$ at different values of R/h and the parameter of heterogeneity γ are shown in Table 1. As is seen, at an appropriate choice of sampling surfaces, a good agreement between calculation results and the analytical solution [23] can be achieved using the Ritz method with the members retained in the expansion of displacements in power series expressed in terms of the transverse coordinate, which corresponds to 11 sampling surfaces inside the shell. The choice of 13 sampling surfaces provides from 9 to 11 correct significant figures for the basic vibration frequency. We

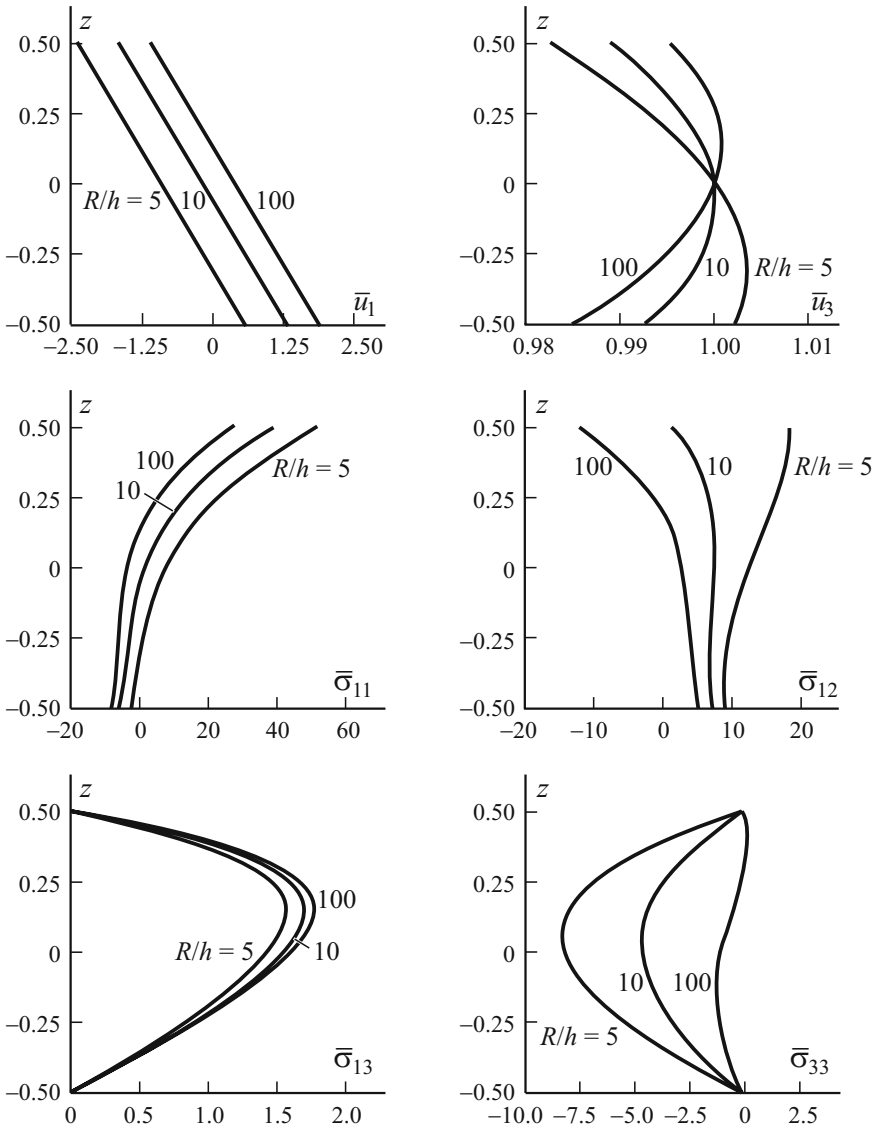

Fig. 2. Distributions of displacements and stresses across the thickness of a cylindrical metal-ceramic shell at $N = 11$, $\gamma = 2$, $r = s = 1$, and $q = 1$; the eigenfrequencies $\bar{\omega}_{11}^{(1)}$ for the chosen values of R/h are given in Table 1.

should also note that a further increase in the number sampling surfaces to 23 increases the calculation accuracy only insignificantly.

From Table 2, it is visible that the choice of 15 sampling surfaces already results in six correct significant figures for the stresses corresponding to the basic vibration mode, except for the transverse normal stresses, for which a greater number of sampling surfaces is required.

On Figs. 2 and 3, the distributions of displacements and stresses across the shell thickness is illustrated at different numbers of half-waves in the longitudinal and transverse directions in the case of 11 sampling surfaces for shells with a parameter of heterogeneity $\gamma = 2$ and different values of the parameter R / h. The results found point to a high potential of the high-order theory of shells suggested, because the boundary conditions on shell faces for the transverse components of stress

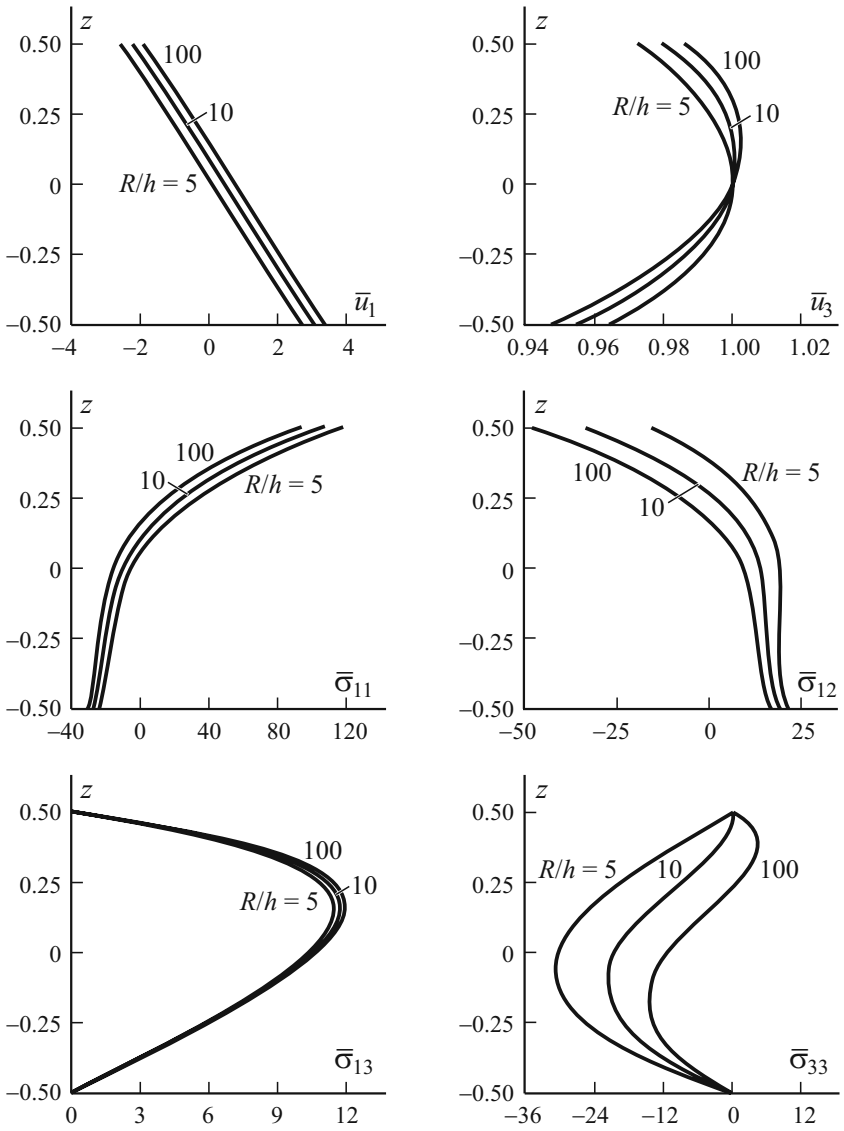

Fig. 3. Distributions of displacements and stresses across the thickness of a cylindrical metal-ceramic shell at $N = 11$, $\gamma = 2$, $r = s = 2$, and $q = 1$; the eigenfrequencies $\bar{\omega}_{22}^{(1)}$ = 102.11, 100.11, and 100.30 correspond to R/h = 5, 10, and 100, respectively.

tensor are satisfied with a high accuracy. In addition, on Fig. 4, the logarithmic error $\delta_{i3}^{\pm} = \log\left|\bar{\sigma}_{i3}(\pm 0.5)\right|$ of boundary conditions is shown for the transverse stresses on the internal and external surfaces of shells in the case of a great number of sampling surfaces. The continuous curves correspond to the results obtained in the case where roots of the Chebyshev polynomial were chosen as interpolation nodes, but the dash-dotted ones were constructed based on the approach with equidistant sampling surfaces [11-13]. Thus, the second approach does not ensure a monotonous convergence of the computing process and can result in an inadequate description of the stress state of shells in the zone of edge effect if high-degree Lagrange interpolation polynomials are used.

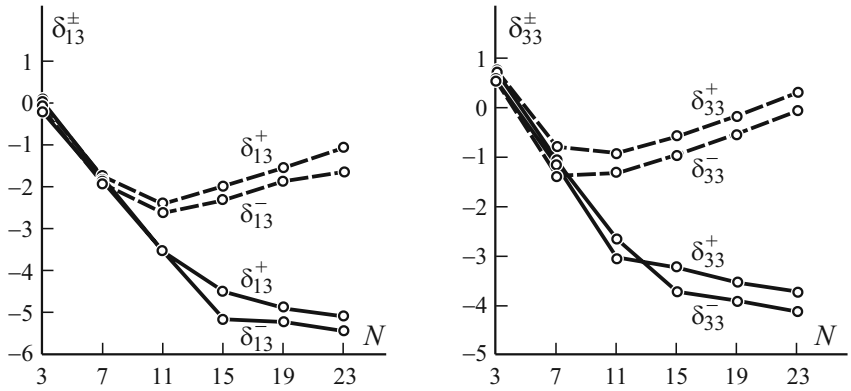

Fig. 4. Logarithmic errors $\delta_{i3}^{\pm} = \log\left|\bar{\sigma}_{i3}(\pm 0.5)\right|$ of boundary conditions for the transverse strain on the internal and external surfaces of a shell with $R/h = 10$ and $\gamma = 2$ $r = s = q = 1$. Explanations in the text.

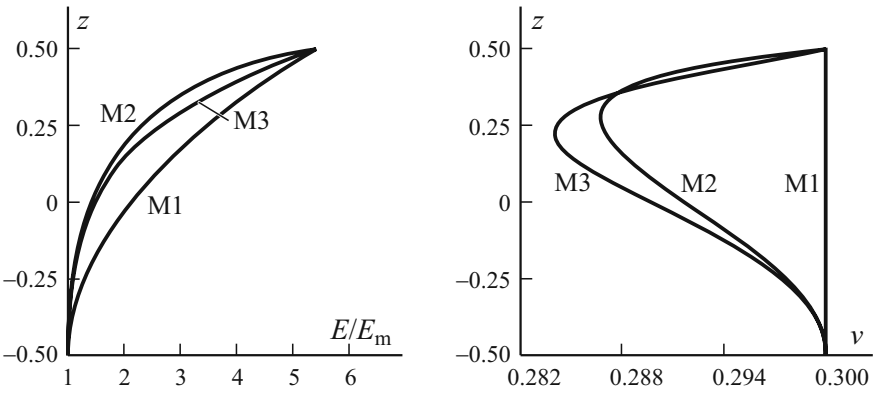

Fig. 5. Distributions of the elastic modulus and Poisson ratio across the thickness of a cylindrical metal-ceramic shell at $\gamma = 2$ given by the rule of mixtures (M1), Mori–Tanaka model (M2), and the Hill model (M3). (These designations are also for Figs. 6-8).

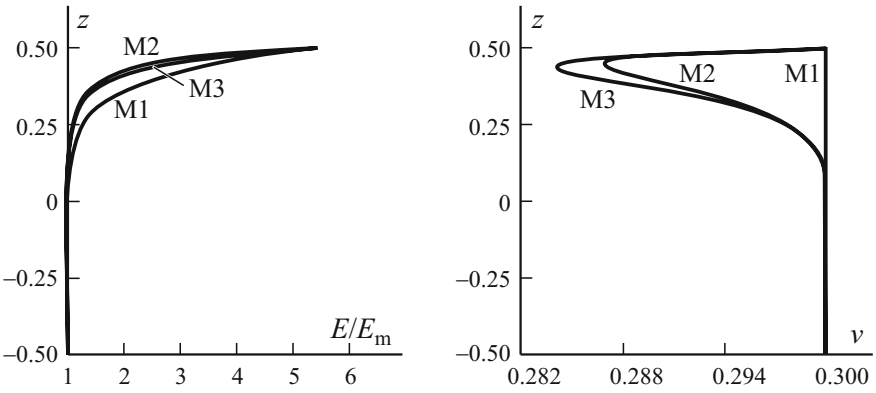

Fig. 6. Distributions of the elastic modulus and Poisson ratio across the thickness of a cylindrical metal-ceramic shell at $\gamma = 10$.

TABLE 3. Calculation Results for the First Eight Frequencies $\bar{\omega}_{11}^{(q)}$ of a Cylindrical Metal-Ceramic Shell with $R/h = 10$, $N = 11$, and Different Values of γ

Model	$\bar{\omega}_{11}^{(1)}$	$\bar{\omega}_{11}^{(2)}$	$\bar{\omega}_{11}^{(3)}$	$\bar{\omega}_{11}^{(4)}$	$\bar{\omega}_{11}^{(5)}$	$\bar{\omega}_{11}^{(6)}$	$\bar{\omega}_{11}^{(7)}$	$\bar{\omega}_{11}^{(8)}$
				$\gamma = 2$				
Rule of mixtures	34.687	144.59	241.41	886.57	908.52	1613.1	1789.2	1824.7
Hill	32.079	131.23	217.68	782.58	804.23	1407.3	1613.8	1639.8
Mori–Tanaka	31.139	125.95	209.05	767.72	788.66	1382.0	1570.7	1597.7
				$\gamma = 10$				
Rule of mixtures	28.568	110.29	183.84	666.74	687.42	1211.1	1365.6	1391.4
Hill	27.188	104.58	173.76	656.55	675.60	1190.4	1326.0	1353.4
Mori–Tanaka	26.716	102.90	171.02	655.73	674.19	1189.3	1323.3	1350.7

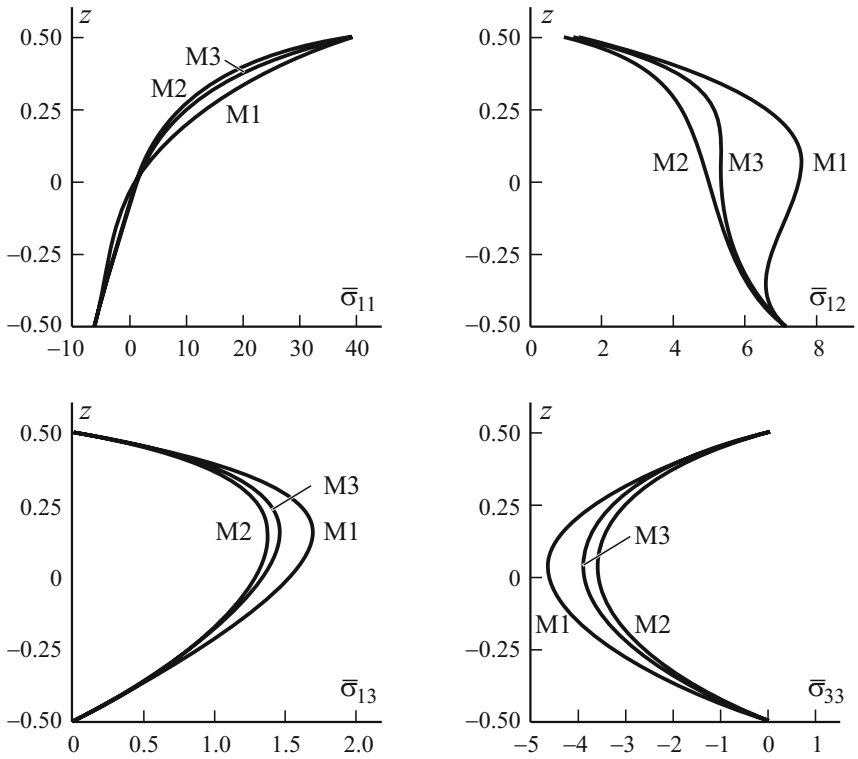

Fig. 7. Distributions of stresses across the thickness of a cylindrical metal-ceramic shell with $N = 11$, $R/h = 10$, $\gamma = 2$, and $r = s = q = 1$.

Finally, let us analyze the free vibrations of a cylindrical shell using the models considered for describing the mechanical characteristics of a metal-ceramic composite at different values of the parameter of heterogeneity γ. On Figs. 5 and 6, distributions of the elastic modulus and Poisson ratio across the thickness of metal-ceramic shells at $\gamma = 2$ and 10 calculated by the rule of mixtures and the Mori–Tanaka and Hill models are shown. As is seen, at a high value of the parameter of heterogeneity, the Mori–Tanaka and Hill models give rather close results. This conclusion is supported by the data given in Table 3

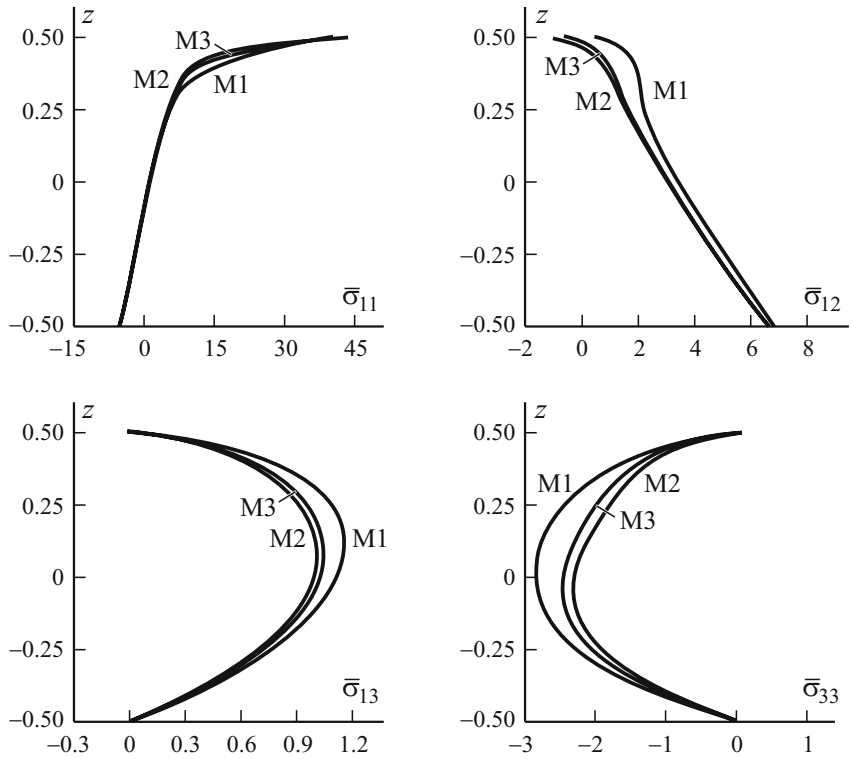

Fig. 8. Distributions of stresses across the thickness of a cylindrical metal-ceramic shell with $N = 11$, $R/h = 10$, $\gamma = 10$, and $r = s = q = 1$.

and also in Figs. 7 and 8, where the distribution of stresses, corresponding to the basic vibration mode, across the shell thickness is shown in the case of 11 sampling surfaces.

Conclusion

The method of sampling surfaces and its application to the solution of the 3D problem on free vibrations of a cylindrical shell made of functional materials has been considered. According to this method, inside the shell body, sampling surfaces parallel to its median surface and passing through the roots of a Chebyshev polynomial are selected in order to take their displacements as required functions. This enables one to find analytical solutions of 3D dynamic problems for composite metal-ceramic shells with a prescribed accuracy, because the solutions obtained asymptotically approach the solutions of 3D elasticity theory.

Acknowledgement. This investigation was supported by the Russian Scientific Fund (project No. 15-19-30002) and the Ministry of Education and Sciences of the Russian Federation (project No. 9.4914.2017/BY).

REFERENCES

1. Z. Q. Cheng and R. C. Batra, "Three-dimensional thermoelastic deformations of a functionally graded elliptic plate," Composites: Part B, **31**, 97-106 (2000).
2. J. N. Reddy and Z. Q. Cheng, "Three-dimensional thermomechanical deformations of functionally graded rectangular plates," Europ. J. Mech. Solids, **20**, 841-855 (2001).
3. J. N. Reddy and Z. Q. Cheng, "Frequency of functionally graded plates with three dimensional asymptotic approach," J. Eng. Mech., **129**, 896-900 (2003).
4. S. S. Vel and R. C. Batra, "Three-dimensional exact solution for the vibration of functionally graded rectangular plates," J. Sound Vib., **272**, 703-730 (2004).
5. S. S. Vel, "Exact elasticity solution for the vibration of functionally graded anisotropic cylindrical shells," Composite Struct., **9**2, 2712-2727 (2010).
6. Y. Ootao and Y. Tanigawa, "Three-dimensional solution for transient thermal stresses of an orthotropic functionally graded rectangular plate," Composite Struct., **80**, 10-20 (2007).
7. A. Alibeigloo and K. M. Liew, "Free vibration analysis of sandwich cylindrical panel with functionally graded core using three-dimensional theory of elasticity," Composite Struct., **113**, 23-30 (2014).
8. V. Birman and L. W. Byrd, "Modeling and analysis of functionally graded materials and structures," Appl. Mech. Rev. **60**, 195-216 (2007).
9. D. K. Jha, T. Kant, and R. K. Singh, "A critical review of recent research on functionally graded plate," Composite Struct., **96**, 833-849 (2013).
10. K. Swaminathan, D. T. Naveenkumar, A. M. Zenkour, and E. Carrera, "Stress, vibration and buckling analyses of FGM plates - A state-of-the-art review," Composite Struct. **120**, 10-31 (2015).
11. G. M. Kulikov and S. V. Plotnikova, "Solution to a problem of statics for an elastic shell in a 3D statement," Reports of the Russian Academy of Sciences, **439**, No. 5, 613-616 (2011).
12. G. M. Kulikov and S. V. Plotnikova, "On the use of a new concept of sampling surfaces in shell theory," Adv. Structured Mater., **15**, 715-726 (2011).
13. G. M. Kulikov and S. V. Plotnikova, "A metod of solving three-dimensional problems of elasticity for laminated composite plates," Mech. Compos. Mater., **48**, No.1, 23-36 (2012).
14. G. M. Kulikov and S. V. Plotnikova, Solution of three-dimensional problems for thick elastic shells on the basis of the method sampling surfaces, Mekh. Tverd. Tela, No. 4, 54-64 (2014).
15. N. S. Bakhvalov, Numerical Methods. Vol.1. [in Russian], M., Nauka, 1973.
16. G. M. Kulikov and S. V. Plotnikova, "Three-dimensional exact analysis of functionally graded laminated composite plates," Adv. Structured Mater., **45**, 223-241 (2015).
17. G. M. Kulikov and S. V. Plotnikova, "A sampling surfaces method and its implementation for a 3D thermal stress analysis of functionally graded plates," Composite Struct., **120**, 315-325 (2015).
18. G. M. Kulikov and S. V. Plotnikova, "Three-dimensional analysis of metal-ceramic shells by the method of sampling surfaces," Mech. Compos. Mater., **51**, No. 4, 647-660 (2015).
19. G. M. Kulikov, S. V. Plotnikova, and A. A. Mamontov, "Sampling surfaces formulation for thermoelastic analysis of laminated functionally graded shells," Meccanica, **51**, No. 8, 1913-1929 (2016).
20. T. Mori and K. Tanaka, "Average stress in matrix and average elastic energy of materials with misfitting inclusions," Acta Metallurgica, **21**, 571-574 (1973).
21. Y. Benveniste, "A new approach to the application of Mori–Tanaka's theory in composite materials," Mech. Mater., **6**, 147-157 (1987).

22. R. Hill, “A self-consistent mechanics of composite materials,” J. Mech. Phys. Solids, **13**, 213-222 (1965).
23. F. A. Fazzolari and E. Carrera, “Refined hierarchical kinematics quasi-3D Ritz models for a free vibration analysis of doubly curved FGM shells and sandwich shells with a FGM core,” J. Sound Vib., **333**, 1485-1508 (2014).